Anomalous Fermi-Surface Dependent Pairing in a Self-Doped High-T_c Superconductor

Yulin Chen,[1] Akira Iyo,[2] Wanli Yang,[1] Xingjiang Zhou,[1] Donghui Lu,[1] Hiroshi Eisaki,[2] Thomas P. Devereaux,[3] Zahid Hussain,[4] and Z.-X. Shen[1]

[1]*Department of Physics, Applied Physics, and Stanford Synchrotron Radiation Laboratory, Stanford University, Stanford, California 94305, USA*
[2]*National Institute of Advanced Industrial Science and Technology, Tsukuba, Ibaraki, 305-8568, Japan*
[3]*Department of Physics, University of Waterloo, Waterloo, Ontario, Canada N2L 3G1*
[4]*Advanced Light Source, Lawrence Berkeley National Laboratory, Berkeley California 94720, USA*

(Received 14 June 2006; published 5 December 2006)

We report the discovery of a self-doped multilayer high T_c superconductor $Ba_2Ca_3Cu_4O_8F_2$ (F0234) which contains distinctly different superconducting gap magnitudes along its two Fermi-surface sheets. While formal valence counting would imply this material to be an undoped insulator, it is a self-doped superconductor with a T_c of 60 K, possessing simultaneously both electron- and hole-doped Fermi-surface sheets. Intriguingly, the Fermi-surface sheet characterized by the much larger gap is the electron-doped one, which has a shape disfavoring two electronic features considered to be important for the pairing mechanism: the van Hove singularity and the antiferromagnetic $(\pi/a, \pi/a)$ scattering.

DOI: 10.1103/PhysRevLett.97.236401 PACS numbers: 71.38.−k, 74.72.Jt, 79.60.−i

The origin of the very high superconducting transition temperature (T_c) in the ceramic copper oxide superconductors is often quoted as one of the great mysteries in modern physics. Important insights on high-T_c superconductivity are often gained through investigations on new compounds with unusual properties. The recently synthesized single crystalline $Ba_2Ca_3Cu_4O_8F_2$ (F0234) is one such example. While valence charge counting based on the canonical chemical formula puts Cu valence as 2^+ thus the material as a half-filled Mott insulator, the compound turns out to be a superconductor with T_c of 60 K [1,2]. We performed high resolution angle-resolved photoemission spectroscopy (ARPES) measurements on this compound. Our data reveal at least two metallic Fermi-surface (FS) sheets with volumes equally above and below half-filling. We also found that the two FS pieces split significantly along the nodal direction which is very different from other multilayer cuprates [3]. Most interestingly, we found an anomalous FS dependence of the superconducting gap in which the larger gap associates with the most bonding FS that lies further away from the antiferromagnetic reciprocal lattice zone boundary and the van Hove points. This discovery puts a strong constraint on theory.

The crystal structure of $Ba_2Ca_3Cu_4O_8(O_\delta F_{1-\delta})_2$ is shown in Fig. 1(a). It has tetragonal symmetry with alternate stacking of superconducting layers (SCLs) and charge reservoir layers (CRLs). Within a conventional unit cell, there are four CuO_2 SCLs that can be divided into two crystallographically inequivalent groups: the outer pair of CuO_2 planes (OP) with apical F atoms and the inner pair (IP) without. As shown in Fig. 1(d), depending on the apical O/F substitution ratio, the superconducting transition temperature (T_c) varies and can reach 105 K when $\delta = 0.4$ [2]. F0234($\delta \approx 0$), the material studied in this investigation, has a $T_c \approx 60$ K.

ARPES experiments were carried out on F0234 samples by using 55 eV photons as described before [4]. The single crystalline samples were grown under high pressure [2]. Total (convolved) energy resolution of the measurements was 16 meV; and the angular resolution was 0.2 deg. Spectra presented in this paper were measured at 20 and 80 K, and the Fermi energy (E_f) is internally referenced to the leading edge position at the d-wave node within each set of data.

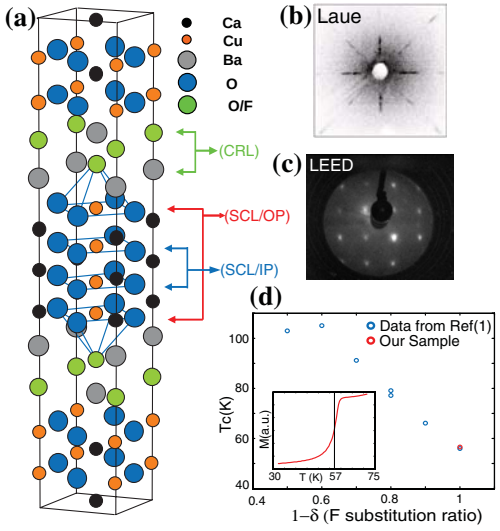

FIG. 1 (color). (a) Crystal structure of $Ba_2Ca_3Cu_4O_8(O_\delta F_{1-\delta})_2$. There are four CuO_2 layers in a unit cell with the outer two having apical F atoms (b) Laue pattern of the sample shows the tetragonal symmetry without superstructure. (c) LEED pattern on the cleaved surface after ARPES measurement confirms no surface reconstruction. (d) T_c vs F-substitution ratio with SQUID measurement of the measured sample (inset).

Submitted to Phys.Rev.Lett.

Work supported in part by the US Department of Energy contract DE-AC02-76SF00515

Figure 2 shows data recorded at 20 K that revealed two sets of distinct bands and FS sheets. The spectral intensity map in Fig. 2(a) is a typical way to illustrate the FS topology. Because of the opening of the superconducting gap, the energy integration window is chosen from 20 meV binding energy (E_b) to Fermi energy (E_f). At the first glance at plot 2(a), it looks similar to other cuprate superconductors [3,5–8], which in general show holelike topology around $(\pi/a, \pi/a)$ in k space, and the intensity peaks along $(0,0) - (\pi/a, \pi/a)$ nodal direction. However, a closer look at the data reveals the presence of at least two dispersive bands (marked as P and N, respectively), which are clearly discernible in both the momentum distribution curves (MDCs) stack plots [2(c) and 2(d)] and the image plots [2(e) and 2(f)] from data cuts illustrated by green arrows in plot 2(a). From 2(c)–2(f), we see that the double peak structures bifurcate further when the two bands disperse to lower binding energy until being limited by the superconducting gap which is more pronounced for band N. The MDC derived dispersions, obtained by fitting the MDC with two Lorentzian peaks plus linear background, are superimposed on plots 2(e) and 2(f), revealing dispersion kinks at $E_b \sim 85$ meV. We see that the kink of band N is stronger than that of band P; and both are stronger in cut 2 [plot 2(f)] than in cut 1 [plot 2(e)]. To show the validity of the fitting procedure at high binding energy, in the inset of Figs. 2(e) and 2(f), we illustrate one (above) and two (below) Lorentzian peaks fits for MDC at $E_b = 150$ meV. It is clear that one Lorentzian peak cannot fit the MDC line shape well.

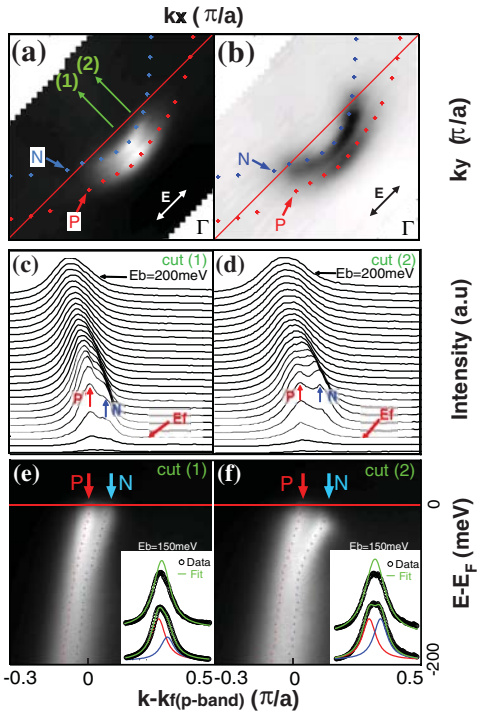

FIG. 2 (color). (a) FS map ($T = 20$ K) by integrating spectral intensity from $E_b = 20$ meV to E_f. White double arrow shows photon polarization. Red and blue symbols give FS contours of bands P and N extracted by the method described in text. (b) Derivative map by integrating the derivative of the spectral density from $E_b = 20$ meV to E_f. Red and blue symbols are defined as in (a). (c)–(f) MDC (c),(d) and image (e),(f) plots of raw data along cuts marked by green arrows in (a). Arrows in (c),(d) show the P and N contributions in MDC curves. Band maxima (k_f) positions are indicated by arrows in (e),(f) marked as P and N, respectively. Dotted lines superimposed on (e),(f) are MDC fit dispersions of both bands. Insets in (e),(f) illustrate one (above) and two (below) Lorentzian peaks fits of the MDCs at $E_b = 150$ meV.

The presence of the two bands can be seen, but not very distinct in Fig. 2(a) because of the large gap magnitude of band N in the region away from the node and the overlapping with the P band close to the node. As another mapping technique, Fig. 2(b) shows a derivative map by integrating the derivative of the spectra intensity within the same energy window as in Fig. 2(a). Because the derivative emphasizes the spectral weight change at the leading edge, it is more sensitive in detecting band-top positions, thus the FS contours. As expected, the two bands' FS contours become more distinct in Fig. 2(b).

The same behavior can be seen in Fig. 3 with data taken at another measuring geometry (see inset). The presence of two sets of bands is self-evident in the raw data image plot and the energy distribution curve (EDC) stack plot in both k-space quadrants. We highlight the EDCs at the band maxima (k_f) positions for one set of bands in the EDC stack plots for clarity. It is obvious from these data that the

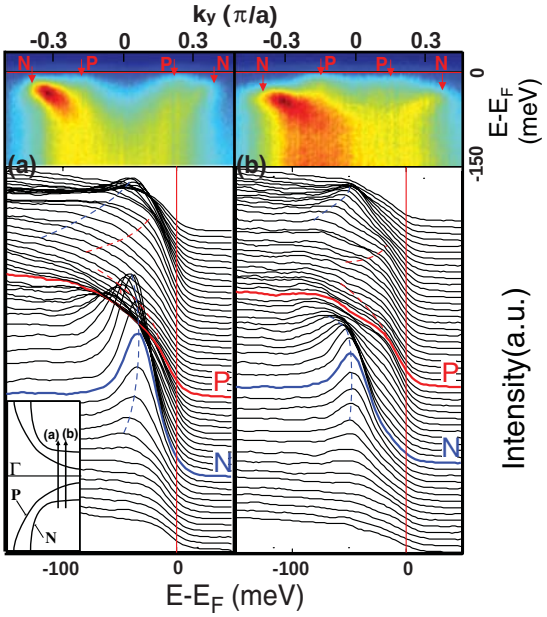

FIG. 3 (color). Raw data image (top) and EDC stack (bottom) plots along cuts indicated in the inset. Red and blue broken lines in EDC plots are guides to the eye that follow the band dispersions. Red and blue bold EDCs represent the EDCs at k_f positions for a pair of P and N bands, which are also indicated by arrows in the image plots.

gap of band N is larger than that of band P as we will discuss in detail later.

To quantitatively determine the FS contours of both bands, we use EDC and MDC analysis complimentarily [9]. We first fit every EDC in each cut to locate the k_f positions for both bands based on the minimum superconducting gap criteria [10] then cross check by fitting MDCs for consistency. The FS contours acquired from sample 1 are superimposed on Figs. 2(a) and 2(b), and those from sample 2 are shown in Fig. 5(a). If we calculate the FS volumes enclosed by each FS sheet with respect to $(\pi/a, \pi/a)$ point within each quadrant [see Fig. 5(a)], we get 0.61 ± 0.04 [unit $(\pi/a)^2$] for band P FS and 0.4 ± 0.03 for band N FS.

In the conventional band structure framework, both FS sheets are holelike. The presence of multiple FS sheets is caused by hybridization of bands from different CuO_2 planes. Similar to an earlier investigation on another multilayer system [11], the number of the bands observed is less than expected from the number of CuO_2 planes. The fact that we see only two FS sheets rather than four as expected indicates that the additional splitting may be too small to be resolved. Compared to what was observed in $Bi_2Sr_2CaCu_2O_8$ (Bi2212) [12,13], we find that the splitting of the FS around the nodal direction is significantly larger.

However, in terms of doped Mott insulator description as is generally used in the field, if we compare our result to the half-filling state in which the FS should have an area of 0.5 in each quadrant, we find that the band P is ''hole-doped'' and the band N is ''electron-doped'': the reason for them being marked as P and N, respectively. Under the convention established for the cuprates, these two pieces of FS are approximately $20 \pm 8\%$ hole- and $20 \pm 6\%$ electron-doped [14], respectively, although the nominal composition indicates F0234($\delta = 0$) to be an undoped Mott insulator. This is the first self-doping case observed in the cuprates.

The self-doping behavior, or significant FS splitting because of inter-CuO_2 plane interaction, while apparently surprising, is consistent with the band structure calculations where the areas of various FSs in multilayer materials are often found to be very different [15–17]. Layer dependent doping has been observed in other multilayer high T_c superconductors such as $HgBa_2Ca_nCu_{n+1}O_{2n+2}$ ($n = 2, 3$) and (Cu,C) $Ba_2Ca_nCu_{n+1}O_{3n+2}$ ($n = 2, 3, 4$), where NMR study showed that the inner CuO_2 layer(s) is less hole-doped than the outer layers [18,19]. We note here that in our F0234 case, both bands are highly metallic with sharp peaks and gap opening below T_c.

It would be very interesting to perform other experiments such as NMR or c-axis optics to test whether this system, with the FS areas quite far away from half-filling and with multilayer interaction, can be better described by the band structure language or the doped Mott insulator language described above. Nevertheless, the isolation of the two FSs allows us to investigate the FS dependence of the superconducting gap, which results in important conclusions independent of the language used.

In Fig. 4, we present the temperature dependent EDCs from various Fermi crossing points of both bands (see inset) that demonstrate the opening of the superconducting gap below T_c. Because of the simultaneous presence of band N, EDCs at points e and f appear broader and show a hump at higher binding energy. It is clear that the spectral intensity of both bands is pushed away from E_f in the $T = 20$ K data compared to those measured at 80 K. The strong temperature dependence suggests the superconducting nature of the energy gaps along both FS sheets at $T < T_c$. Furthermore, we find that the gap magnitude is not only FS sheet dependent (points e, f vs points c, d) but also momentum dependent within each FS sheet (points a–d; e, f).

The FS contours and superconducting gaps along them are summarized in Fig. 5. To avoid model related complexity, we present the leading edge gap [3,20] along both FS contours. While the leading edge method is known to underestimate the absolute gap magnitude, it does not affect the relative comparison. Figure 5(b) gives the gap values as a function of k-space angle as defined in Fig. 5(a); and Figs. 5(c) and 5(d) show three sample EDCs recorded at 20 K along both FS sheets (from which the corresponding gap values in Fig. 5(b) are extracted). From Fig. 5(b), we see that the gaps along both FS sheets have d-wave symmetry as found in other cuprates; and although the leading edge gap magnitude along the band P FS is comparable to that of purely hole-doped materials such as Bi2212 [3,20], a big surprise comes from the gap magnitude of the ''electron-doped'' band N FS, which is approximately 2 times larger than that of its hole-doped counterpart, and an order of magnitude larger than that of purely electron-doped materials such as $Nd_{2-x}Ce_xCuO_4$ [21–23]. Within the framework of the doped Mott insulator, this behavior of the self-doped system contrasts strongly to the established trend of particle-hole asymmetry for superconductivity in purely electron- or hole-doped systems with the n-type materials having much weaker

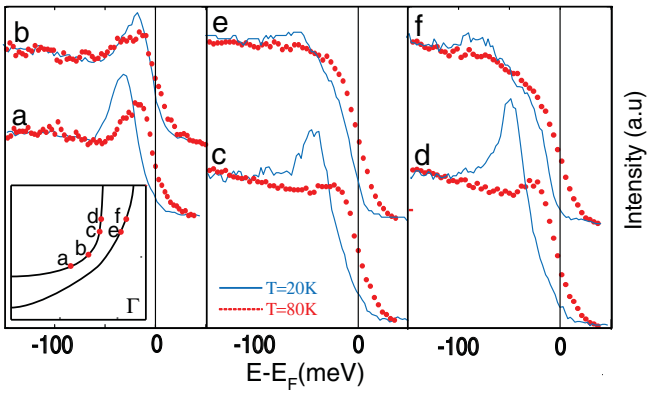

FIG. 4 (color). Temperature dependent EDCs from points a–f along both FSs (see inset); $T = 80$ K(red) and 20 K (blue) data are measured on two cleaves of the same sample.

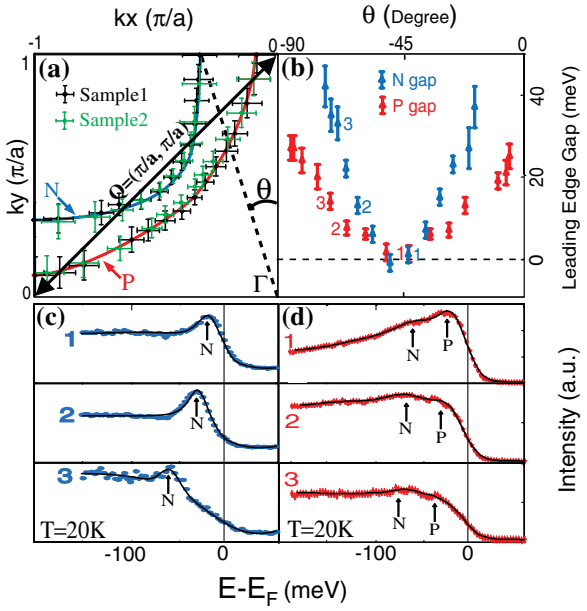

FIG. 5 (color). (a) FS contours from two samples show good agreement. Black double arrow shows the $(\pi/a, \pi/a)$ scattering vector. Angle θ gives the definition of horizontal axis in (b). (b) Leading edge gap along k-space angle from the two FS contours. (c),(d) Three representative EDCs from both FS contours (labeled as 1–3, blue for band N and red for P, respectively, measured at $T = 20$ K) that give the corresponding points in (b). Black lines superimposed on EDCs are empirical fits to the data; the fit peaks' positions from both bands are indicated by black arrows.

pairing strength [21–23]. Unlike the Bi2212 system with bilayer splitting where two FSs are also observed [24,25], F0234 shows nondegenerated FSs even along the nodal direction [see Figs. 2(a)–2(c) and 2(e), Fig. 5(a)] and significant gap difference associated with different FSs. The implications of this difference have been discussed elsewhere [26]. This makes F0234 the first self-doping high T_c superconductor that has a pronounced FS dependence of the superconducting gap.

The substantially larger pairing gap in the energy dispersion along band N FS (see Figs. 2 and 3,) strongly hints that the most important pairing force for cooper pairs is distinct from those theories where the van Hove singularity (VHS) near E_f [27] or antiferromagnetic $(\pi/a, \pi/a)$ scattering [28] are the most important ingredients. As seen in Fig. 5(a), though band N never and band P does get close to $(\pi/a, 0)$ in k space where the VHS provides a large phase space that can be connected by the $(\pi/a, \pi/a)$ scattering vector, band N nevertheless shows much larger gap. On the other hand, the correlation between a stronger kink and a larger gap in band N may imply a connection. While this does not exclude the possibility that VHS and $(\pi/a, \pi/a)$ scattering from playing some role in the superconducting pairing [29], our finding strongly suggests that there exists a more important mechanism in this material.

On the other hand, our finding is consistent with the empirical trend which indicates that it is the FS shape of the most bonding band that correlates with T_c [30]. As an example, $HgBa_2Ca_2Cu_3O_8$, the superconductor with the highest T_c(135 K) to date, is predicted [31] to have its most bonding band's FS similar to that of band N in F0234.

We thank J. Zaanen, N. Nagaosa, and O. K. Andersen for stimulating discussions. The experiments were performed at the ALS of LBNL, which is operated by the DOE's Office of BES, Division of Material Science, with Contract No. DE-AC03-76SF00098. The division also provided support for the work at SSRL with Contract No. DE-FG03-01ER45929-A001. The work at Stanford was supported by NSF Grant No. DMR- 0304981. T. P. D. acknowledges support from NSERC and ONR Grant No. N00014-05-1-0127.

[1] A. Iyo *et al.*, Physica (Amsterdam) **392C–396C**, 140 (2003).
[2] A. Iyo *et al.*, Supercond. Sci. Technol. **17**, 143 (2004).
[3] A. Damascelli, Z. Hussain, and Z.-X. Shen, Rev. Mod. Phys. **75**, 473 (2003).
[4] X. J. Zhou *et al.*, J. Electron Spectrosc. Relat. Phenom. **142**, 27 (2005).
[5] D. S. Marshall *et al.*, Phys. Rev. Lett. **76**, 4841 (1996).
[6] H. Ding *et al.*, Phys. Rev. Lett. **76**, 1533 (1996).
[7] S. V. Borisenko *et al.*, Phys. Rev. Lett. **84**, 4453 (2000).
[8] T. Yoshida *et al.*, Phys. Rev. Lett. **91**, 027001 (2003).
[9] T. Valla *et al.*, Science **285**, 2110 (1999).
[10] H. Ding *et al.*, Phys. Rev. Lett. **78**, 2628 (1997).
[11] D. L. Feng *et al.*, Phys. Rev. Lett. **88**, 107001 (2002).
[12] D. L. Feng *et al.*, Phys. Rev. Lett. **86**, 5550 (2001).
[13] Y. D. Chuang *et al.*, Phys. Rev. Lett. **87**, 117002 (2001).
[14] Relative doping is calculated from the FS area in each quadrant by the following formula: $100\% \times$ [(FS area)-0.5]/0.5.
[15] W. E. Pickett, Rev. Mod. Phys. **61**, 433 (1989).
[16] O. K. Andersen *et al.*, J. Phys. Chem. Solids **56**, 1573 (1995).
[17] N. Hamada and H. Ihara, Physica (Amsterdam) **357C–360C**, 108 (2001).
[18] Y. Tokunaga *et al.*, Phys. Rev. B **61**, 9707 (2000).
[19] H. Kotegawa *et al.*, Phys. Rev. B **69**, 014501 (2004).
[20] Z.-X. Shen *et al.*, Phys. Rev. Lett. **70**, 1553 (1993).
[21] N. P. Armitage *et al.*, Phys. Rev. Lett. **86**, 1126 (2001).
[22] T. Sato *et al.*, Science **291**, 1517 (2001).
[23] Q. Huang *et al.*, Nature (London) **347**, 369 (1990).
[24] P. V. Bogdanov *et al.*, Phys. Rev. Lett. **89**, 167002 (2002).
[25] S. V. Borisenko *et al.*, Phys. Rev. B **66**, 140509 (2002).
[26] W. Xie *et al.*, cond-mat/0607198.
[27] R. S. Markiewicz, J. Phys. Chem. Solids **58**, 1179 (1997).
[28] A. Abanov, A. V. Chubukov, and J. Schmalian, Adv. Phys. **52**, 119 (2003).
[29] V. S. Oudovenko, S. Y. Savrasov, and O. K. Andersen, Physica C (Amsterdam) **336**, 157 (2000).
[30] E. Pavarini *et al.*, Phys. Rev. Lett. **87**, 047003 (2001).
[31] D. J. Singh, Phys. Rev. B **48**, 3571 (1993).